

Experimental analysis of operational data for roundabouts through advanced image processing

*Original*

Experimental analysis of operational data for roundabouts through advanced image processing / Mussone, L., Bassani, M.. - In: JOURNAL OF TRAFFIC AND TRANSPORTATION ENGINEERING. - ISSN 2095-7564. - STAMPA. - (2019).  
[10.1016/j.jtte.2019.01.005]

*Availability:*

This version is available at: 11583/2743124 since: 2019-07-22T15:49:54Z

*Publisher:*

Elsevier

*Published*

DOI:10.1016/j.jtte.2019.01.005

*Terms of use:*

This article is made available under terms and conditions as specified in the corresponding bibliographic description in the repository

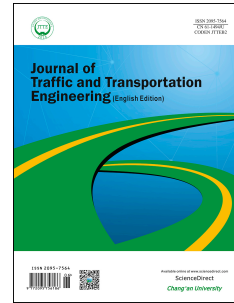
*Publisher copyright*

(Article begins on next page)

# Journal Pre-proof

Experimental analysis of operational data for roundabouts through advanced image processing

Marco Bassani, Lorenzo Mussone



PII: S2095-7564(18)30426-4

DOI: <https://doi.org/10.1016/j.jtte.2019.01.005>

Reference: JTTE 266

To appear in: *Journal of Traffic and Transportation Engineering (English Edition)*

Received Date: 9 September 2018

Revised Date: 22 January 2019

Accepted Date: 28 January 2019

Please cite this article as: Bassani, M., Mussone, L., Experimental analysis of operational data for roundabouts through advanced image processing, *Journal of Traffic and Transportation Engineering (English Edition)*, <https://doi.org/10.1016/j.jtte.2019.01.005>.

This is a PDF file of an article that has undergone enhancements after acceptance, such as the addition of a cover page and metadata, and formatting for readability, but it is not yet the definitive version of record. This version will undergo additional copyediting, typesetting and review before it is published in its final form, but we are providing this version to give early visibility of the article. Please note that, during the production process, errors may be discovered which could affect the content, and all legal disclaimers that apply to the journal pertain.

© [Copyright year] Periodical Offices of Chang'an University. Publishing services by Elsevier B.V. on behalf of Owner.

1 Original research paper

2

## 3 **Experimental analysis of operational data for** 4 **roundabouts through advanced image processing**

5 Marco Bassani<sup>a</sup>, Lorenzo Mussone<sup>b,\*</sup>

6

7 <sup>a</sup> *Department of Environment, Land and Infrastructure Engineering, Politecnico di Torino, Torino 10129, Italy*

8 <sup>b</sup> *Department of Architecture, Built Environment and Construction Engineering, Politecnico di Milano, Milano*  
9 *20133, Italy,*

10

### 11 **Highlights**

- 12 • An investigation carried out to survey vehicle movements at roundabouts was presented.
- 13 • O/D matrix, classification, trajectories tracking, speed and acceleration from video images  
14 analysis.
- 15 • A number of camera set-up configurations were adopted.
- 16 • Performance of installation set-ups with different vehicle tracking strategies has been evaluated.

17

### 18 **Abstract**

19 Roundabout is still the focus of several investigations due to the relevant number of variables affecting  
20 their operational performances (i.e., capacity, safety, emissions). To develop reliable models,  
21 investigations should be supported by devices and related sensors to extract variables of interest (i.e.,  
22 flow, speed, gap, lag, follow-up time, vehicle classification and trajectory). Notwithstanding that  
23 several sensors and technologies are currently used for data collection, most of them present  
24 limitations. The paper presents the investigation carried out to survey vehicle movements at  
25 roundabouts as a comprehensive video image analysis system is able to derive the origin/destination

26 (O/D) matrix, compile a vehicle classification, track individual vehicle trajectories together with  
27 corresponding speeds and accelerations along paths. To this end, the authors collected video-  
28 sequences that were analyzed with a piece of software developed for that task. To minimize the  
29 problems due to perspective distortion, environmental effects, and obstructions, a number of camera  
30 set-up configurations were adopted with equipment being placed on central or external poles, and on  
31 permanent fixtures such as raised working platforms outside the confines of the intersection area.  
32 Performance of those installation set-ups with different vehicle tracking strategies has been evaluated.  
33 Particularly, speed has been successfully related to trajectory tortuosity, the result of which  
34 emphasizes the tremendous potential of image analysis and opens up to further studies on the  
35 evaluation of the operational effects of roundabout geometrics.

36 **Keywords:**

37 Transportation; Roundabout; Image analysis/processing; Vehicle tracking and classification; Operating  
38 speed; Trajectory.

39

40

41

42

43

---

44 \* Corresponding author. Tel.: +39 02 2399 5182; fax: +39 022 399 5195.

45 E-mail addresses: marco.bassani@polito.it (M. Bassani), lorenzo.mussone@polimi.it (L. Mussone).

46

47

48

49

## 50 1 Introduction

51 In many countries, roundabouts have increasingly become the intersection of choice due to the  
52 positive and acknowledged operational benefits deriving from their geometrics as reported in literature  
53 (Curti et al., 2008; Rodegerdts et al., 2010, 2014). Nevertheless, operational performance in terms of  
54 capacity, speed, and safety still remains a focus of investigation due to the number of variables, apart  
55 from geometric ones, affecting trajectories and speeds of crossing vehicles (Sacchi et al., 2011), and  
56 emissions (Fernandes et al., 2015; Salamati et al., 2013).

57 With the objective of developing reliable models, investigations should be conducted using  
58 robust tools and with attention being paid contextually to the circulating roadway and all the legs.  
59 Such tools have to be able to: (a) extract traffic variables of interest such as flow, speed, gap, lag,  
60 follow-up time, vehicle length and weight, as well as vehicle position in time (i.e., vehicular  
61 trajectory); (b) ensure that the recording video system is not visible to drivers so as to avoid any  
62 behavioural effects; and (c) contribute to a reduction in the resources needed to run the system, also  
63 in terms of operator time.

64 Although several sensors and technologies are currently used for traffic data collection in  
65 roundabout, most of them are limited in their ability to survey traffic variables, a point which is  
66 discussed in the paper. In order to avoid the limitations associated with their use, video recording  
67 surveys and related image processing techniques can be successfully employed (Messelodi et al.,  
68 2005; Migliore et al., 2006; Mussone et al., 2013).

69 The paper proposes a methodological contribution to analyse speed and trajectories of vehicles  
70 through roundabouts. It presents the activities undertaken by the authors in the development and use  
71 of a video recording system in conjunction with a software developed for the derivation of: (a) the  
72 origin/destination (O/D) flow matrix, (b) the vehicle classification, and (c) the trajectories and  
73 associated speeds and curvature diagrams along the paths traversing a roundabout.

74

## 75 2 Background

### 76 2.1 *Vehicle position data collection tools*

77 At present, many multi-purpose detectors for traffic data collection are available at affordable prices.  
78 Laser, radar, microwaves, infrared, acoustic, ultrasonic, capacitive, piezoelectric, magnetometric, and  
79 magnetic loops are the technologies employed in sensors. With more or less similar levels of  
80 efficiency and precision, all the above-mentioned technologies allow for the collection of macroscopic  
81 variables such as flow, speed, density (or occupancy) and vehicle specific variables such as headway,  
82 gap, lag, follow-up time and vehicle length and weight.

83 Their main disadvantage (apart from the fact that they sometimes need to be physically supported  
84 or that, in some cases, their installation can occasionally lead to an intrusion into the traffic circulation  
85 area) is that their measurements refer to a single road section or linear segment, and therefore  
86 multiple measurement points require an array of collection tools. None of them, in fact, may be  
87 employed for vehicle tracking, especially in situations where vehicles move along inflected trajectories  
88 (e.g., in case of roundabouts). This would not be a serious problem unless it is strictly necessary that  
89 information gathered by detectors relates uniquely to each individual vehicle. This task is particularly  
90 crucial at roundabouts where the construction of the O/D matrix is very challenging (Grenard and Wei,  
91 2012).

92 One possible way to track vehicles could be the floating car data method that, however, requires  
93 that a statistically significant number of vehicles are equipped with positioning sensors i.e., global  
94 positioning system-global navigation satellite system (GPS-GNSS), inertial measuring unit (IMU) or  
95 combined sensors, with data recorded on board and/or transferred to a central system. With this  
96 method, installations and experiments are expensive and complicated since it (the method) needs a  
97 large number of vehicles together with the participation of the general public to be of any use in a  
98 realistic setting. However, the current wide diffusion of navigation systems working in real time and  
99 connected to a central unit makes this feature of increasing interest for the near future, at least for  
100 transport planning purposes (average speed prediction and O/D matrix reconstruction). Other  
101 emerging survey technologies, such as the 3D light detection and ranging (LiDAR), facilitate the

102 collection of clouds of data and could be used to track vehicles. At present, however, they are more  
103 expensive than video-image technology and entail a higher level of complexity and effort in the  
104 collection and modelling of a large quantity of data.

105 Consequently, the most promising methodology available at present for the tracking of vehicles is  
106 certainly represented by the video analysis technique. Several contributions have demonstrated that it  
107 may be employed in a variety of applications from simple vehicle detection (Messelodi et al., 2005;  
108 Wei et al., 2005) to the gathering of comprehensive data for trajectories in both time and space  
109 domains, thus allowing a complete reconstruction of movements along sections (Beymer et al., 1997)  
110 and at vehicle intersections (Alhajyaseen et al., 2013; Apeltauer et al., 2015; Datondji et al., 2016;  
111 Dinh and Tang, 2017; St-Aubin et al., 2013) or cyclist behaviour trajectory analysis (Sakshaug et al.,  
112 2010; Zaki et al., 2013).

113 With the aim of providing information useful for the calibration of microscopic simulation models,  
114 Alhajyaseen et al. (2013) analysed the relationship between speed and trajectory at at-grade urban  
115 intersections. Adopting the survey technique described in Suzuki and Nakamura (2006), those authors  
116 demonstrated the effect on vehicle trajectory of geometry (angles between legs, corner radii, number  
117 of exit lanes, and positions of hard noses of the medians) for different vehicle types negotiating the  
118 intersection at different speeds, confirming the potential of the image analysis technique when  
119 conducting surveys to gather positioning data at road junctions. In Mussone (2013), the question of  
120 visibility on roundabouts was faced by using real trajectories extracted from video image records.

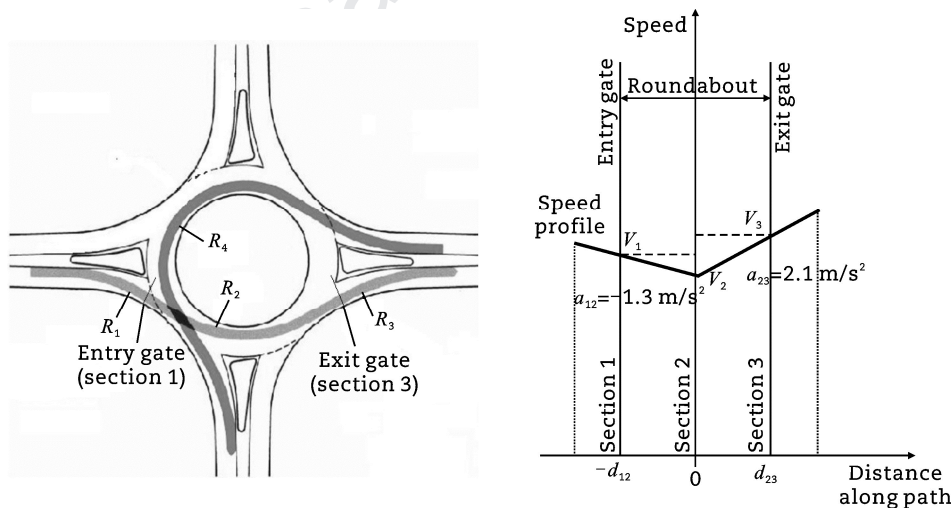
121 Finally, the possibility to track vehicles in roundabouts by video cameras mounted on drones has  
122 raised a certain interest. Guido et al. (2016) used them to detect and compare tracking data with GPS-  
123 equipped vehicles only. According to the authors, the methodology is promising but needs to be  
124 improved for removing noise and inaccuracies due to uncontrolled movements and vibrations of  
125 drones under the effects of wind.

## 126 *2.2 Position and speed data modelling at roundabouts*

127 Operational data for modern roundabouts were investigated for the first time in the National  
128 Cooperative Highway Research Program (NCHRP) Project 3-65, when a comprehensive inventory of

129 103 US roundabouts with geometric, operational, and safety data was carried out (Rodegerdts et al.,  
 130 2007). Of these, 31 roundabouts were the focus of video recordings in the spring and summer of 2003,  
 131 with 34 h of traffic operation data accumulated (i.e., flow measurements, gaps, delays and travel times,  
 132 turning movement proportions, and vehicle types). For this purpose, a video recording system  
 133 consisting of analogic and digital video cameras was used. Operational data were recorded making  
 134 use of "event recording" software (Rodegerdts et al., 2006). In the same study, sixteen single-lane and  
 135 eleven multi-lane roundabouts were considered for the operating speed surveys (Fig. 1).

136 In Rodegerdts et al. (2007), speed data were collected through the use of radar guns only at four  
 137 specific locations: one outside (i.e., at 60 m from the yield line) and three inside the roundabouts. In  
 138 particular, as seen in Fig. 1, they were collected at the yield line (section 1), at the midpoint of the  
 139 adjacent splitter island (section 2), and at the exit (section 3), with a minimum number of speed data  
 140 per section greater than 30 to achieve a statistical significance. Speed data collected at the  
 141 roundabouts were differentiated both by movement type (i.e., left, through or right turn), and by vehicle  
 142 type (i.e., passenger cars, trucks), and only passenger car data were used for that analysis.



143

144 **Fig. 1** Layout of the operating speed surveys (Rodegerdts et al., 2010). (a) Geometric characteristics of trajectories. (b) Schematic speed  
 145 profile.  
 146

147 Starting from the elementary arc with the minimum radius on which the minimum speed is reached  
 148 in the circulatory roadway ( $V_2$ ), speeds at the entry ( $V_1$ ) and exit ( $V_3$ ) gates can be derived under the

149 hypothesis of naturally decelerated/accelerated motion and adopting average deceleration ( $a_{12}$ ) and  
 150 acceleration ( $a_{23}$ ) values from observational data (Robinson et al., 2000).

151 The predictive speed equations (Rodegerdts et al., 2007) for the through movement for entry ( $V_1$ )  
 152 and exit ( $V_3$ ) speeds in km/h (Fig. 1) are

$$153 \quad V_1 = \min \left\{ V_{1\text{base}}; 3.6 \sqrt{\left(\frac{V_2}{3.6}\right)^2 - 2a_{12}d_{12}} \right\} \quad (1)$$

$$154 \quad V_3 = \min \left\{ V_{3\text{base}}; 3.6 \sqrt{\left(\frac{V_2}{3.6}\right)^2 + 2a_{23}d_{23}} \right\} \quad (2)$$

155 where  $a_{12}$  is the deceleration between the point of interest of the entry path and the midpoint of the  
 156 path (assumed equal to  $-1.3 \text{ m/s}^2$ ),  $a_{23}$  is the acceleration between the midpoint of the path and the  
 157 point of interest of the exit path (assumed equal to  $2.1 \text{ m/s}^2$ ), and  $d_{12}$  and  $d_{23}$  are the distances  
 158 between the points of interest along the entry and exit paths, and the midpoints of these paths  
 159 respectively, which are measured along the vehicle trajectory. In Eqs. (1) and (2),  $V_{1\text{base}}$ ,  $V_2$  and  $V_{3\text{base}}$   
 160 represent the predicted speeds at the entry, midpoint and exit points based on path radii  $R_1$ ,  $R_2$  and  $R_3$   
 161 (Fig. 1) using the basic formula of vehicle equilibrium on curves (Eq. (3)).

$$162 \quad \begin{cases} V_{1\text{base}} = \sqrt{gR_1(f+q)} \\ V_2 = \sqrt{gR_2(f+q)} \\ V_{3\text{base}} = \sqrt{gR_3(f+q)} \end{cases} \quad (3)$$

163 where  $g$  is the acceleration of gravity (equal to  $9.81 \text{ m/s}^2$ ),  $f$  is the side friction factor, and  $q$  is the  
 164 super-elevation, which is normally  $-2\%$  in the case of modern roundabouts (Rodegerdts et al., 2007).

165 Eq. (3) may also be used to evaluate the speed along a left turn movement, using the value of  $R_4$   
 166 indicated in Fig. 1 as a radius.

167 A comparison between the 85th percentile speed observed in the field and the corresponding  
 168 values predicted using Eqs. (1) and (2) demonstrated that the proposed model was applicable to  
 169 those maneuvers in which vehicles interact with the central island (left turn and through movements),  
 170 and that it was considered conservative because it tends to overestimate the operating speed. The  
 171 regression analyses performed on these models with available data showed the coefficients of  
 172 determination to be too low, thus indicating that the variables considered could not provide a reliable

173 prediction of speed on the circulatory roadway. This leads to the conclusion that the evaluation of  
174 operating speed at roundabouts still remains a challenge at both the analysis level and design stage  
175 (Šurdonja et al., 2018; Perco et al., 2012).

176 Currently, TORUS (Transoftsolutions, 2018) and CIVIL 3D (Autodesk, 2018) software packages  
177 consider the fastest path analysis according to literature (Robinson et al., 2000; Rodegerdts et al.,  
178 2007). These programs calculate the expected speed on the circulatory roadway along the minimum  
179 radius along the “fastest vehicle path”, which represents the smoothest possible trajectory of a vehicle,  
180 in the absence of other vehicles and ignoring all lane markings, from the entry to the exit gates (Ahac  
181 et al., 2016; Rodegerdts et al., 2006).

### 182 **3 Methodology**

183 Starting from this literature review, the authors proposed a comprehensive methodology to collect  
184 video records from existing roundabouts and derive information useful to model the relationship  
185 between speeds and trajectories of vehicles. The tracking of trajectories gives also the possibility for  
186 the derivation of trajectory tortuosity parameters, as well as the reconstruction of O/D matrix. From the  
187 length of moving objects in the road scene, a neural network was trained to classify vehicles along  
188 each movement.

189 To minimize the problems due to perspective distortion, environmental effects, and obstructions, a  
190 number of camera configurations were adopted with equipment being placed on central or external  
191 poles (with respect to central island), or on permanent fixtures such as raised working platforms  
192 outside the confines of the intersection area. Strengths and weaknesses of the selected installations  
193 are described in order to determine the optimal set-up. Three case studies in Northern Italy were  
194 considered. Up to three video cameras were used in different set-ups. Each installation exhibited a  
195 different behaviour under the effects of wind, cloud cover, shadows, dazzle, perspective deformation,  
196 and obstructions. Two additional aspects, namely ease of perspective correction and synchronization  
197 between video cameras, were also investigated and solved.

198 An important issue faced in the paper is the synchronization of recorded images when using more  
199 than one video camera. This was achieved by inserting a timestamp for every recorded stream. This

200 task is easier when cameras are mounted on the same pole and camera output can be connected  
201 directly to the same computer. More demanding is the case when several cameras on different poles  
202 are involved and a wireless connection is needed to link the computers together to use the same  
203 timestamp. Besides this, the authors experimented two different strategies in order to build trajectories:  
204 by merging trajectories extracted by separated images (MT) and blending images before extracting  
205 trajectories (BI).

206 Finally, the data collected from image analysis in the three case studies have provided general  
207 relationships between speeds and trajectories as affected by roundabout geometrics. Differently from  
208 the approach of Robinson et al. (2000) and Rodegerdts et al. (2007), continuous speed and trajectory  
209 data help the authors in the development of a new model able to relate speeds to trajectory tortuosity.  
210 The possibility to work out such a model can be considered by analysts and designers as an  
211 opportunity to predict speed behaviour of drivers along their path on the basis of roundabout  
212 geometrics.

### 213 *3.1 Survey tools and methodology*

214 The instrumentation used to collect and evaluate data consists of a vision system and a real time  
215 kinematics-global positioning system (RTK-GPS), both connected to a dedicated PC (Fig. 2). In  
216 Mussone et al. (2011, 2013), a more detailed description of the system, including details of both  
217 hardware and software characteristics, can be found. Images from video cameras must not have blind  
218 spots and this condition can be achieved through a planned set up of optics and video camera  
219 orientation.

220 The vision system (Fig. 2(a)) consists of one to three cameras with a resolution of 1360 x 1024  
221 pixels. The optical lens of each video camera was adjusted in line with the application scenario by  
222 remote control. The vision system provided information on vehicular flow through the processing of  
223 images recorded by the video camera(s), while the RTK-GPS system was used to generate data  
224 useful for calibrating and evaluating the vision system.

225 The RTK-GPS system (Fig. 2(b)) is composed of a base station equipped with a Trimble MS750  
226 GPS and a Trimble Zephyr Antenna. A rover, made up of a Trimble 5700 GPS (working at 5 Hz) and a

227 Trimble Zephyr Antenna, is attached to a probe vehicle and connected via radio link (DiGi XBee Pro  
228 modules in point to point mode) to the base station.

229

230 (a)



(b)



231

232 **Fig. 2** Data collection and evaluation instrumentation. (a) Vision system placed upon a raised working platform. (b) The probe vehicle  
233 with the rover system.

234

235 In order to improve the process of matching video camera data with GPS data, a series of marked  
236 points visible in video images were drawn on the pavement surface of the roundabout (four points on  
237 each leg, and from four to eight points on the circulatory roadway depending on the dimension(s) of  
238 the central island). The exact positions of these points were, then, attained by both GPS (with an  
239 accuracy ranging from 2 to 15 cm) and by video recording. The matching of vehicle coordinates (and  
240 then speed) data calculated by image processing with the data gathered by GPS was then a relatively  
241 straightforward task.

242 Calibration of the vision system was carried out for image rectification, thus tuning the Bouguet  
243 camera model of the vision system. Image rectification aims at achieving homogeneity in terms of  
244 corresponding pixels in the image plane, and the ratio between lines lengths and angles in a specific  
245 plane of the observed world (i.e., the central islands is circular but it appears an ellipse in the  
246 perspective projection). This requires a proper image transformation, i.e., a homography between the  
247 road surface and the image plane. Vehicle tracking on the transformed plane turns out to be quite

248 effective and more accurate than when carried out on the original image. The homography is known  
249 when the size and the position of some specific elements of the observed scene are available.

### 250 3.2 *Pre processing*

251 The images gathered require conversion, undistortion, and rectification, while RTK-GPS data need  
252 data conversion (for rover data) and synchronization between base station and rover timestamps.

253 The image analysis was carried out by a software (developed at Politecnico di Milano and based on  
254 MATLAB platform) named Vehicle Tracking for Roundabout Analysis (VeTRA), which employs genetic  
255 algorithm optimization procedures to minimize the re-projection error of the central island onto the  
256 image plane, and also provides a complete projective transformation from the 3D real world to the 2D  
257 image, by constraining world points to lie at ground level.

258 The current version of VeTRA has further improved performance in blob recognition with respect to  
259 the original version used in Mussone et al. (2011). Improvements to the algorithms have now limited  
260 the negative effects of some environmental factors (i.e., wind, sudden changes in light conditions due  
261 to clouds), occlusions due to fixed objects (i.e., trees, poles) and moving vehicles (Oh et al., 2012), as  
262 well as perspective deformations.

263 The key tool in VeTRA is its tracking system, which detects moving objects in the field through an  
264 adaptive background modelling and subtraction algorithm. The image areas representing the vehicles  
265 (known as “blobs” in information science jargon) are identified in the foreground through shadow and  
266 noise removal. The tracking system is capable of distinguishing between newly detected blobs and  
267 previously tracked vehicles between three types of vehicles as explained in the next paragraph. The  
268 blobs are continuously updated as new information is received. All these activities rely on a proper  
269 model of the background, which has to be sufficiently robust to contend with daily changes in light  
270 conditions and camera oscillations. Although the tracking system detects the movements of objects in  
271 the background, it is able to filter and hence exclude from computation all the small movements of any  
272 objects (i.e., trees, sheets on the pavement, etc.) affected by wind.

273 When more than one video camera is used, two different strategies can be employed to consolidate  
274 the information. One strategy merges the blob trajectories extracted from each separate video image

275 (here called Merging Trajectory (MT) strategy), the second blends images from video cameras before  
276 extracting trajectories from the blended images (here called Blend Images (BI) strategy). There are a  
277 number of problems and advantages associated with each strategy that were tested in this experiment.

278 With the MT strategy, the trajectory of the same vehicle is extracted from video cameras (two or  
279 more) as in the approach with one camera only. After that, trajectories of the same vehicle are  
280 associated and superimposed in order to obtain only one trajectory. The challenging activity is the  
281 association of trajectories avoiding strong discontinuities between them.

282 With the BI strategy, a new image is generated from the blending of all images collected to exclude  
283 the portions of images affected by distortion. Then, blended images are analysed as in the one  
284 camera approach to extract trajectories.

285 The MT strategy makes it easier to extract blob trajectories separately from each video camera but  
286 does not guarantee a perfect continuum (in the sense of function derivability) of single trajectories. On  
287 the other hand, the BI strategy allows a final complete trajectory which is perfectly continuous but  
288 requires considerable effort due to merging images. In fact, isomorphic transformation and  
289 perspective correction must be applied to each image to maintain the same scale over the trajectory.

290 It is worth noting that new set-ups with a different number of video cameras required an  
291 improvement of the original version of VeTRA (Mussone et al., 2013). The new images produced by  
292 blending separate images, or the new trajectories derived from mixing the trajectories given by each  
293 video camera, are significant results for the post processing phase.

### 294 3.3 *Post processing I – trajectory reconstruction*

295 For each video survey, the blob trajectories produced by the tracking system are processed and  
296 stored in a database in order to generate the O/D matrix, vehicle trajectories, speed profiles and the  
297 vehicle classification.

298 Trajectories on pavement surfaces are calculated from trajectories between the entry and exit gates  
299 of the circulatory roadway on the image plane using RTK-GPS data collected by the rover on the  
300 probe vehicle. This was accomplished through a comparison of RTK-GPS and tracking system data,  
301 using the synchronization data to obtain the same amount of information. Extracted trajectories are

302 then saved to a system of local coordinates. Speed and curvature profiles are obtained from  
303 calculations based on vehicle position and time. Speed is calculated for two consecutive points by  
304 simply dividing the distance between them by the elapsed time (equal to the frame rate of the camera,  
305 except in those very rare cases where some frames have been lost).

306 The tracking system used in VeTRA follows two different procedures. The first one is less  
307 sophisticated and is employed for flow classification purposes as it distinguishes between (a) bikes  
308 and motorbikes, (b) light vehicles, vans and campers, and (c) heavy vehicles. It detects the blob for  
309 each vehicle, which is then tracked from the entry to the exit section. In this paper, only classes (b)  
310 and (c) were used for performance comparison since too few bikes and motorbikes were observed  
311 during the survey.

312 Classification is based on vehicle dimension, particularly on its length, which is derived from blob  
313 length. Since blob dimension generally changes according to its position inside the image (that is, the  
314 position inside the circulatory roadway) due to perspective distortion, a neural network (NN) was used  
315 to classify vehicle length by using for training some images sampled from vehicle trajectory,  
316 accurately divided by movements. The NN must be trained in every location because it needs to learn  
317 the effect of perspective distortion along the circulatory roadway. The accuracy of NN recognition was  
318 high with an error lower than 3% for trajectories closer to video camera; higher errors were observed  
319 for short trajectories, and for those farther from the video camera where perspective distortions may  
320 create difficulties in recognition.

321 The second tracking procedure is more accurate and is employed for trajectory and speed analysis.  
322 It recognizes the barycentre (or centroid) of each blob in 2D and produces a continuous curve formed  
323 by points that are known in the space and time domains. More details on tracking procedures are  
324 available in Mussone et al. (2013).

### 325 *3.4 Post processing II – data treatment for speed analysis*

326 A filtering algorithm in VeTRA was included to reject trajectories in which the speeds are too low due  
327 to vehicle conflict both in the circulatory roadway and in the approaching and departure legs. More  
328 specifically, vehicles that stopped before entering or reduced the speed to give priority to circulating

329 ones were excluded from the speed analysis to obtain free flow speeds only. As a result, trajectories  
 330 with average speeds between entry and exit lower than 10 km/h were discarded. Filtering was also  
 331 necessary to exclude stationary vehicles in the circulating roadway, or affected in trajectory by  
 332 conflicting vehicles. In fact, in some cases, very low speeds were the result of superimposition of  
 333 trajectories (and blobs) of two or more vehicles.

334 When available in time and space domains, the trajectory of any isolated vehicle traversing the  
 335 roundabout in free-flow conditions contains all the information necessary for an assessment of how  
 336 the said vehicle trajectory was affected by the geometry of the roundabout. Tortuosity indexes may be  
 337 used to characterize curved trajectories. In this paper, two tortuosity indexes, having as an objective  
 338 the characterization of the vehicle paths associated with specific maneuvers (crossing, right, left and  
 339 U-turn), have been derived by reference to general literature. It is obvious that these indexes cannot  
 340 capture all aspects of driver behaviour but they are helpful in understanding whether the trajectory  
 341 itself and related vehicular speed are confined to a range within recommended operating intervals.

342 According to Fig. 3, the first index ( $T_1$ ) (a derivation of index  $T_2$ , presented hereafter) is shown as  
 343 follow

$$344 \quad T_1 = \sum_i (|\alpha_i|/R_i)/L \quad (4)$$

345 where  $|\alpha_i|$  is the absolute value of the angle between the tangents passing from two successive  
 346 recorded points ( $P_i$  and  $P_{i+1}$ ,  $P_{i+1}$  and  $P_{i+2}$ ),  $R_i$  is the radius of the osculating circle that is derived from  
 347 thirty points around the considered one (15 before  $-P_{i-15}$ ,  $\dots$ ,  $P_i$ , and 15 after  $-P_{i+1}$ ,  $\dots$ ,  $P_{i+15}$ ),  $L$  is the  
 348 length of the trajectory between the entry and the exit gates, and  $i$  is one of the considered points. The  
 349 sum over  $i$  includes all the points between the entry and the exit gates. Thirty-one points allow to  
 350 manage a set of images of one second duration (at the current frame rate), which can be considered  
 351 long enough to smooth peaks due to random noise effects in blobs.

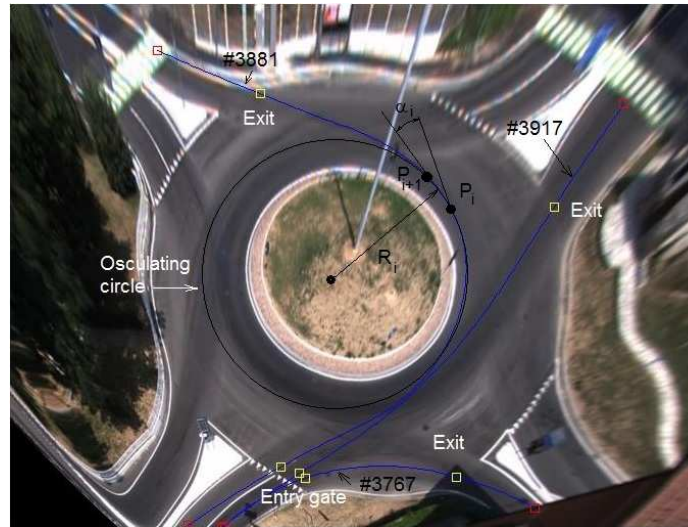
352 The second tortuosity index ( $T_2$ ) is obtained with the Eq. (5).

$$353 \quad T_2 = \sum_i (|\alpha_i|/L) \quad (5)$$

354 Eq. (5) is also known in literature as the curvature change ratio (Yasser and Mohamed, 2011).

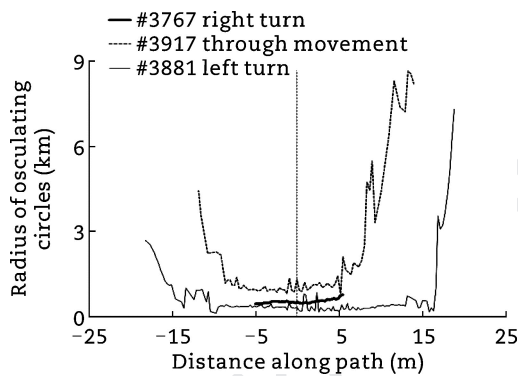
355

356 (a)



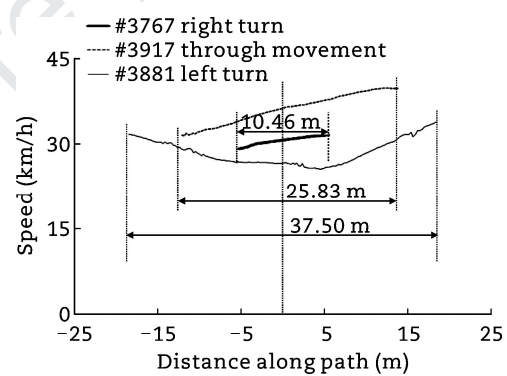
357

358 (b)

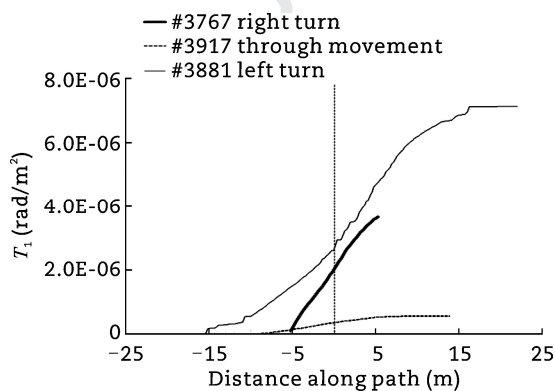


359

360 (c)



361 (d)



362

363

364

365

366

(e)

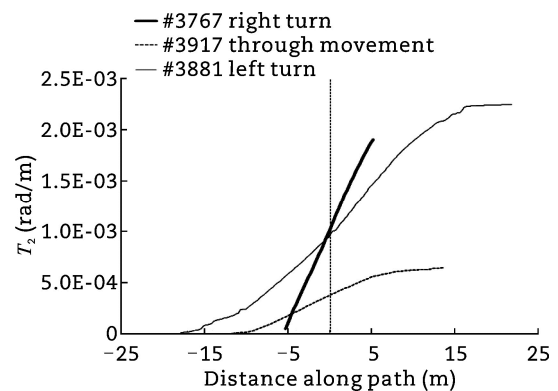


**Fig. 3** Trajectory analysis. (a) Typical curves for parameter analysis. (b) Trajectory radius. (c) Speed. (d)  $T_1$ . (e)  $T_2$ .

Fig. 3 shows the typical curves for the four parameters extracted from trajectory analysis (trajectory radius, speed, and two tortuosity indices) for three main movements: right, through and left turn (U-

367 turn was not considered due to the paucity of data examples). In the same Fig. 3, the cumulated  
368 values of these two indexes from the initial point at the entry gate ( $i = 1$ ) to the generic points ( $i$ ) along  
369 the trajectory is also plotted.

370 The two indexes indicate the level of difficulty in negotiating the roundabout, which is higher when  
371 the angles are high and the corresponding radii are small. The units of measurement for the two  
372 tortuosity indexes are  $\text{rad/m}^2$  and  $\text{rad/m}$ , respectively. In Fig. 3(d) and (e), they have been plotted  
373 according to the formulas with values that increase along the travelled path, for three trajectories  
374 selected from the Biella roundabout database (each identified with a 4-digit code). In Fig. 3(b) and (c),  
375 for the same three trajectories, the radius of the osculating circles and the speed profile are plotted. It  
376 is worth noting that in Fig. 3, the central point of the path has a reference station equal to 0.

377 As previously indicated, the speed at each of the  $P_i$  points along a generic trajectory is calculated by  
378 simply dividing the distance between every point  $P_i$  and the consecutive point  $P_{i+1}$  by the elapsed time  
379 (equal to the frame rate of the video camera that was equal to 0.0333 s). For the radius diagram,  
380 thirty-one consecutive points of the trajectory (resulting in 1 s of images) have been considered for the  
381 estimation of  $R_i$  values.

#### 382 4 Investigation

383 With a view to establishing the optimal camera configuration and assessing the performance of  
384 VeTRA, in-field research activities were initially undertaken at five roundabouts in northern Italy  
385 (Piedmont and Lombardy regions), chosen for their geometrical characteristics and environment (rural  
386 and urban). Table 1 reports a synthesis of the geometric characteristics and the most significant  
387 survey data, while Fig. 4 illustrates three general video camera configurations used for the surveys.

388 Unfortunately, two other sites with different set-ups and in urban environment were investigated but  
389 recorded images were unusable due to the effects of a strong wind in one case and to a reflected  
390 dazzle in the latter that were not possible to remove.

391 Images were recorded for between 1.5 and 2 h to obtain at least one hour of actual flow. The  
392 recording period was in and around the peak hour of midday and, in all cases, the weather conditions  
393 were prevalingly dry and sunny with occasional passing clouds.

394 The first roundabout is located near the urban limits of the city of Biella (Fig. 5, with the identification  
 395 of tracked vehicles, entry and exit gates, and video camera direction (arrow)), and connects two  
 396 arterials with two lanes per direction and separated carriageways.

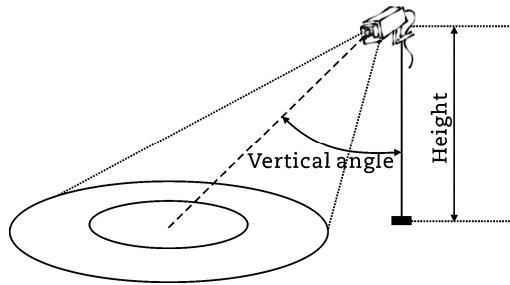
397 Pedestrian crossings are provided at three of the four legs. The external diameter is 50 m, the  
 398 circulatory roadway is 13 m in width, while the central island diameter is equal to 24 m including a  
 399 truck apron of 1.5 m. The approaching legs have two lanes with an average width of 8 m, while 6 m is  
 400 the width of the single lane departure legs. The roundabout is equipped with a lighting tower headlight,  
 401 while the water harvesting systems are located outside the circulatory roadway. During the study, the  
 402 detection system was placed on a moveable rack near the edge of the southwest corner. The video  
 403 camera, pointing towards the centre of the roundabout, was placed at a height of about 22 m at an  
 404 angle of approximately  $55^\circ$  with respect to the rack axis.

405 **Table 1** Synthesis of information for survey activities.  
 406

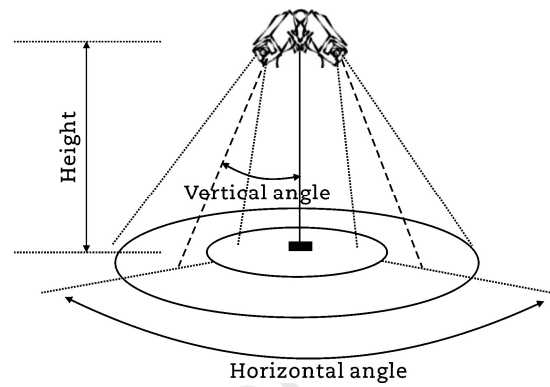
Roundabout	Biella	Ghisalba	Poncarale
Latitude	45°33'12".39	45°35'32".21	45°27'29".99
Longitude	8°04'21".85	9°46'19".75	10°12'09".66
Inscribed diameter, $D_{INS}$ (m)	50	46	70
Inner island diameter, $D_{INT}$ (m)	24	26	56
Circulatory roadway width, $W_{CR}$ (m)	13	10	7
Number of legs	4	4	4
Configuration # (Fig. 4)	1	2	3
Number of cameras	1	3	3
Manufacturer	Goyo GM12314S	No.2 Goyo GM12314S (2.30 mm, 94°)	Goyo GM12314S
(focal length, FOV)	(2.30 mm, 94°)	No.1 Theia MY125M (1.43 mm, 125°)	(2.30 mm, 94°)
Number of survey points	1	1	2
Video camera position	External	Internal	External
Horizontal angle (°)	-	90	120
Vertical angle (°)	55	40	72 (1 camera) 55 (2 cameras)
Camera height (m)	22	22	32

407 Note: FOV is field of view.  
 408  
 409

410 (a)



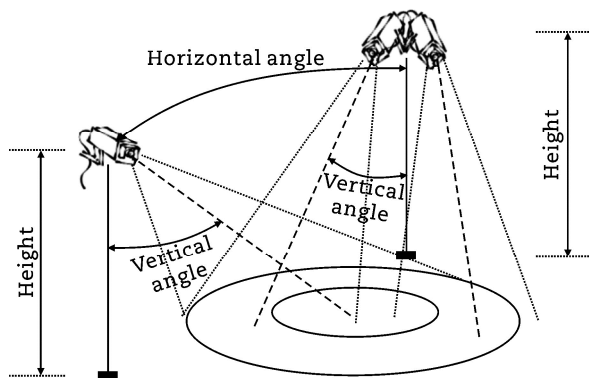
(b)



411

412

413 (c)



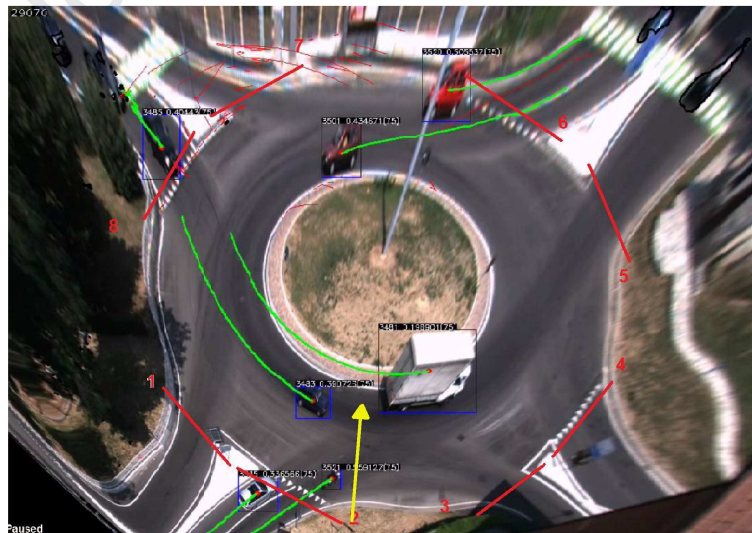
414

415

416

417

**Fig. 4** Scheme of the three video camera configurations adopted for the survey. (a) Configuration #1. (b) Configuration #2. (c) Configuration #3.



418

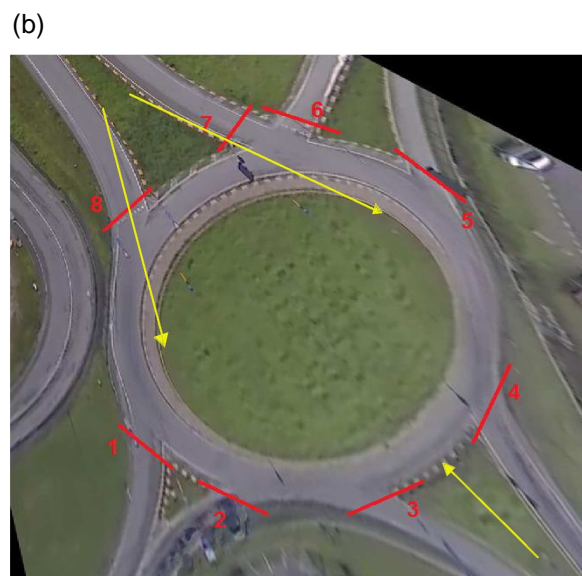
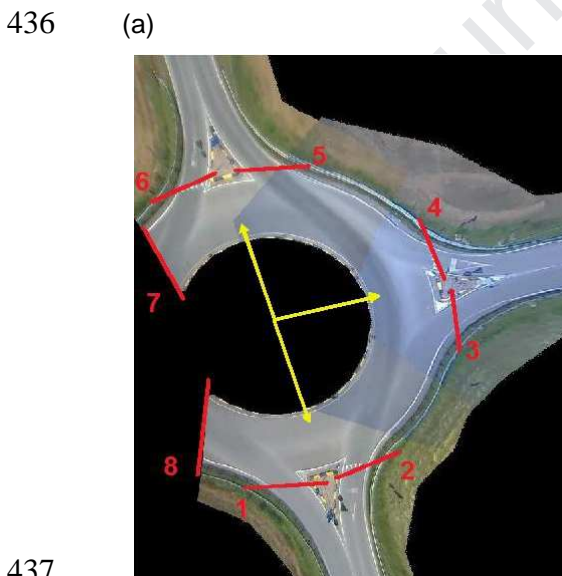
419

420

**Fig. 5** Aerial view of the Biella roundabout.

421 The second roundabout is located in a rural area near Ghisalba (Fig. 6(a)) at the intersection of two  
 422 single-carriageway rural highways with no pedestrian crossings. The external diameter is 46 m, the  
 423 circulatory roadway is 10 m, and the central island diameter is equal to 26 m with a truck apron of 2 m.  
 424 The roundabout is furnished with a central lighting tower headlight. The detection system, consisting  
 425 of three cameras, was placed on the lighting pole in the centre of the central island at a height of  
 426 about 21 m above the roundabout plane, with the three cameras facing east, north and west  
 427 respectively and placed at vertical angles of approximately  $40^\circ$  with respect to the pole.

428 The third roundabout lies outside the urban area of Poncarale (Fig. 6(b)) at the intersection of two  
 429 main highways, both of which are single carriageway with two-way traffic and no pedestrian crossings.  
 430 The external diameter is equal to 70 m and the circulatory roadway is only 7 m. As a result, the  
 431 roundabout has a wide central island (56 m in diameter) that includes a truck apron of 2.5 m. In  
 432 contrast with the other two roundabouts, the approaching and departure legs of the Poncarale  
 433 roundabout are tangent to the circulatory roadway. The lighting is provided by two lighting towers,  
 434 located on two divisional islands to the north and south, distant 81 and 28 m respectively from the  
 435 roundabout.



437  
 438 **Fig. 6** Aerial view of roundabouts. (a) Ghisalba roundabout. (b) Poncarale roundabout. (Arrows indicate video-camera direction).

439 The measurements were taken with three cameras installed at a height of 32 m, two of which were  
 440 located on the southern lighting pole at an angle of approximately  $55^\circ$  and the third on the northern

441 lighting pole at an angle of approximately 72°. The cameras were attached to the lifting system to  
442 which the lamps of the central pole are fixed. This system is lifted and lowered whenever lamp  
443 maintenance is conducted. Since the video cameras were close to the lamps, it is reasonable to  
444 assume that they were not seen by drivers and so did not influence their behaviour. Survey vantage  
445 points were determined according to the particular set-up adopted (Fig. 4), with video cameras able to  
446 cover the entire roundabout.

## 447 **5 Results and analysis**

### 448 *5.1 Vehicle classification and O/D matrix*

449 As explained before, the classification of vehicles has been limited to two classes of vehicles (light  
450 and heavy) which, when combined, represent more than 95% of the total observed flow for the three  
451 investigated case studies. Classification is worked out by a neural network previously trained through  
452 a sample of cases which are manually extracted.

453 Using different combinations of the two strategies cited previously (merged trajectories (MT) and  
454 blended images (BI)), the number of video cameras (from one to three (1C–3C)) and configurations  
455 (from #1 to #3), five different cases have been considered and reported in Table 2 to validate the  
456 estimates produced by VeTRA. In Table 2, the results are shown for all the possible sixteen  
457 movements into a 4-leg roundabout, with the last row containing the total number of movements  
458 recorded by VeTRA and the corresponding average values counted by the operators (specifically,  
459 three people who manually counted vehicles looking at the videos and subdividing such counts by  
460 movements).

461 The data elaborated by VeTRA and expressed in percentage terms ( $v_i$ ), calculated on the total  
462 collected flow, were compared with those obtained from video observation by a number of operators.  
463 These measurements are reported in Table 2 in percentage under the column “Operator” ( $o_i$ ), and  
464 were repeated until the average values between observations were significantly stable (i.e., the mean  
465 did not change anymore with the addition of new observations, according to the central limit theorem),  
466 and could be considered a “true” reference. Assuming application of the central limit theorem,

467 repeated extractions (analysis of same video images by the same operator) lead to a reduction in  
 468 error when estimating the mean. It should be noted that the total number of vehicles observed in one  
 469 hour of survey time was high (1500–2500 veh/h).

470 **Table 2** Comparison of percentage values of the O/D matrixes for Biella, Ghisalba and Poncarale roundabouts.  
 471

O/D movement	Biella (configuration #1)		Ghisalba (configuration #2)			Poncarale (configuration #3)		
	Operator (%)	VeTRA (%)	Operator (%)	VeTRA (%)		Operator (%)	VeTRA (%)	
		1C		3C-MT	3C-BI		1C	2C-BI
2-1	0.40	0.59	0.00	0.00	0.00	0.14	0.00	0.10
2-3	2.93	3.37	2.98	4.72	3.56	7.14	4.70	12.02
2-5	20.96	20.33	26.46	23.29	25.89	7.24	3.65	0.10
2-7	0.47	0.44	1.08	1.15	1.47	3.48	1.05	6.11
4-1	3.26	2.49	0.00	0.00	0.00	5.43	5.89	7.46
4-3	0.20	0.26	0.00	0.10	0.05	0.28	0.07	0.10
4-5	4.64	4.80	0.66	1.20	0.95	4.64	7.36	0.10
4-7	7.82	6.87	2.53	2.45	2.61	17.76	18.58	30.05
6-1	19.79	21.13	0.00	0.00	0.00	9.60	12.90	0.00
6-3	4.66	2.60	0.00	0.14	0.00	4.08	4.84	0.00
6-5	0.29	0.00	0.00	0.05	0.00	0.09	0.07	0.00
6-7	7.07	8.68	31.22	30.46	29.98	0.19	0.84	0.21
8-1	2.05	2.71	30.60	31.95	31.54	7.79	8.27	9.12
8-3	11.90	13.27	2.03	2.26	2.19	19.67	27.70	34.09
8-5	13.22	12.24	2.40	2.17	1.71	12.29	3.86	0.00
8-7	0.33	0.23	0.04	0.05	0.05	0.19	0.21	0.52
Total flow (veh)	2002	2060	2415	2078	2105	2156	1706	1154

472  
 473 In this phase, the authors focused mainly on error evaluation rather than on absolute values, so  
 474 Table 2 reports the percentage values for each movement with respect to the total number of  
 475 movements.

476 Bernardin and Stiefelhagen (2008) suggested the use of clear multiple object tracking (MOT)  
 477 metrics to measure the performance of video image processing. It is made up of two indexes: (a) the  
 478 total error value averaged by the number of matches made when estimating position (indicated as  
 479 MOTP–multiple object tracking precision–and discussed in the next subparagraph), and (b) the  
 480 tracking accuracy (MOTA–multiple object tracking accuracy), estimated using the following equation.

481 
$$\text{MOTA} = 1 - (\sum_t (m_t + fp_t + mmc_t)) / (\sum_t g_t) \quad (6)$$

482 where for any time  $t$ ,  $m_t$  is the number of misses,  $fp_t$  is the number of false positives,  $mmc_t$  is the  
 483 number of mismatches, and  $g_t$  is the number of objects.

484 In this application, we calculated MOTA using all data collected by operator but only data for  
 485 completely detected trajectories by VeTRA (since partially revealed trajectories are not of interest in  
 486 this context and then the number of objects,  $g$ , is lower), thus leading to possible worse performance.  
 487 Therefore, the subscript  $t$  (usually the index of each frame) is here assumed to be linked to a whole  
 488 trajectory. This index varies from 1 to 0 (from best to worst performance). Besides, differences  
 489 between operator and VeTRA are firstly calculated for each movement and then summed up. Three  
 490 other different error types were also calculated from Table 2 and listed in Table 3 according to  
 491 performance indexes used in technical literature: the sum of absolute differences ( $E_1$ ), the average of  
 492 absolute differences ( $E_2$ ), and the average of differences ( $E_3$ ).  $E_1$ ,  $E_2$ , and  $E_3$  are calculated according  
 493 to the following equations.

$$494 \quad E_1 = \sum_i |v_i - o_i| \quad (7)$$

$$495 \quad E_2 = \sum_i |v_i - o_i|/n \quad (8)$$

$$496 \quad E_3 = \sum_i (v_i - o_i)/n \quad (9)$$

497 where  $n$  represents the number of movements considered in the analysis.

498 Difference between  $E_1$  and  $E_2$  depends only on the number of movements  $n$  taken into  
 499 consideration but this number may change from site to site. Hence, when comparing performance of  
 500 two sites, it may be useful to use both indexes. Besides the indexes, their percentages were also  
 501 taken into consideration. They were calculated considering  $v_i / \sum_i v_i$  instead of  $v_i$  for  $E_1$ , and  
 502  $o_i / \sum_i o_i$  instead of  $o_i$  for  $E_2$ . For  $E_3$ , the average percentage is always nil.

503 It must be stressed that operators represent the way to obtain the true result by application of the  
 504 central limit theorem. In this experiment, since an infinite number of operators is not possible, the  
 505 calculated averages may be considered a good estimate of the true result. VeTRA results are,  
 506 nonetheless, affected by deterministic errors that cannot be completely avoided since they are  
 507 intrinsic to the system (i.e., video cameras and lenses).

508 Values for the average of the absolute differences (Table 2) between operator and VeTRA  
 509 generated data are less than 5% and are compatible with traffic analysis resolution. This also holds  
 510 true, albeit to a lesser extent, for the average of percentage differences (considering all movements).

511 In contrast, the sum of percentage differences is generally very high even with the best strategy (see  
512 Ghisalba-BI and Biella-1C in Table 2).

513 This last result shows the existence of a bias due to the general set-up conditions during the survey.  
514 The fact that bias is positive indicates that VeTRA has generally estimated a lower percentage value  
515 for each movement than that obtained by the operators. In the cases of Biella and Poncarale, the bias  
516 is positive, while in Ghisalba, it is negative.

517 On examination of the five analyses carried out with VeTRA (Tables 2 and 3), the best results were  
518 obtained with configuration #1 in Fig. 4, in particular when considering the MOTA index. In fact, the  
519 performance obtained with the use of one video camera, which has lower costs and requires less  
520 effort, is quite similar to that of configuration #2 in which three video cameras are employed. Moreover,  
521 in the latter case at least four video cameras would be necessary to ensure adequate coverage of the  
522 entire surface of the roundabout (Fig. 6).

523 The problems resulting from the blending of sequences obtained from three video cameras located  
524 at 32 m from the roundabout (configuration #3 of Fig. 4) led to the necessity of considering two  
525 different strategies in the analysis of the Poncarale roundabout. Although the performance indicators  
526 (in Table 3) in the case of three-camera (Ghisalba-3C) and also a single camera (1C) configurations  
527 are still quite close to those established in the Biella case study, the use of a two-camera (2C)  
528 configuration with blended images results in the worst performance observed.

529 The use of additional cameras can result in operating problems related to factors such as  
530 synchronization between frames from different cameras, different orientations and separated  
531 communication wires. Synchronization is an acute problem that can be exacerbated by the loss of  
532 some frames. In addition, the different orientation of video cameras requires different isomorphisms,  
533 that is, different camera calibrations and homography transformations. The result obtained for  $E_3$  of  
534 Biella, which is indeed very low, is not surprising since Eq. (9) does not use absolute values and  
535 therefore errors, which are not very biased in this case, cancel each other.

536

537

538

539  
540**Table 3** Performance indicators (errors) between operator and VeTRA computed values according to Eqs. (6)-(8).

Roundabout and image treatment strategy	$E_1$		$E_2$		$E_3$	MOTA (%)
	(sum of absolute differences)		(average of absolute differences)		(average of differences)	
	Percentage	Value	Percentage	Value	Value	
	(%)	(veh)	(%)	(veh)	(veh)	
Biella (1C)	11.64	58	0.72	4	0.89	88
Ghisalba (3C-MT)	8.47	419	0.53	26	21.00	82
Ghisalba (3C-BI)	5.03	336	0.31	21	19.00	86
Poncarale (1C)	34.52	643	2.15	41	28.00	70
Poncarale (2C-BI)	75.88	1006	4.74	63	63.00	53

541 *5.2 Positions and speeds validation*

542 Since the distances between the RTK-GPS data and the VeTRA probe vehicle obtained data are not  
543 Gaussian distributed, the MOTP index (Bernardin and Stiefelhagen, 2008) is split into three other  
544 indexes – the median, median of absolute deviations (MAD), and inter-quartile range (IQR) (Table 4).

545 The results are available for the six different analyses carried out on the three roundabouts and the  
546 different strategies of image processing. Furthermore, Table 4 lists the average and the standard  
547 deviation of the speed differences recorded by both the on-board RTK-GPS system and by the  
548 tracking process, for the same combination of roundabout and image processing strategies.

549 The results show that differences in positions and speed occur when different configurations and  
550 processing strategies are adopted. The best performances in terms of tracking were observed in the  
551 following cases: single camera configuration (Biella), two cameras with image blending (2C-BI) and  
552 merged trajectory (2C-MT) strategy (Poncarale). Greater distances between tracked points were  
553 measured when configuration #2 of Fig. 4 with three central cameras was adopted, and in the case of  
554 the survey carried out at Poncarale, where only one camera was used to analyse vehicle movements  
555 at a roundabout with the largest diameter (70 m) between the three here investigated.

556 As regards speeds, the best results in terms of average and standard deviation were noted in the  
557 Biella survey, while the worst performances were those in the Poncarale survey in which the image  
558 analysis procedure was conducted with one camera only. This would suggest the necessity to use  
559 more than one camera for surveys of roundabouts larger than the Poncarale one.

560  
561**Table 4** Distribution of errors in distance and speed difference between VeTRA and RTK-GPS data.

Roundabout	Distance (m)			Speed difference (km/h)	
	Median	MAD	IQR	Average	Standard deviation
Biella (1C)	0.375	0.179	0.399	0.11	2.71
Ghisalba (3C-MT)	0.651	0.457	0.863	0.12	7.31
Ghisalba (3C-BI)	0.272	0.743	0.619	3.06	8.87
Poncarale (1C)	0.576	0.250	0.576	11.46	23.66
Poncarale (2C-MT)	0.383	0.191	0.436	1.06	8.64
Poncarale (2C-BI)	0.384	0.173	0.397	7.58	18.71

562

563 In the case of Poncarale with the strategy 2C-MT, data analysis was limited to speed analysis and  
 564 not extended to the whole set of analyses due to difficulties in building the whole trajectory. In too  
 565 many cases, the continuity of the trajectory curve was not achieved.

### 566 5.3 Tortuosity and speeds analysis

567 An analysis of tortuosity and related speeds was performed on the class of light vehicles only. For  
 568 each trajectory and at each point ( $i$ ), VeTRA derives the two tortuosity indexes and local speeds from  
 569 the recorded positions and times when the centre of the vehicle occupies the points  $i+1$ ,  $i$  and  $i-1$ . All  
 570 the trajectories are grouped under the same O/D maneuver and the software can elaborate the  
 571 requested statistical output selected by the operator.

572 Table 5 contains the synthesis of the 15th percentile of the two tortuosity indexes ( $T_{1,15}$  and  $T_{2,15}$ )  
 573 calculated for those parts of the trajectories including the entry and exit gates of the roundabouts, and  
 574 the 85th percentile of corresponding speeds at: (1) the entry gate ( $V_{1,85}$ ), (2) the midpoint of the  
 575 trajectory inside the circulatory roadway ( $V_{2,85}$ ), and (3) the exit gate ( $V_{3,85}$ ) as indicated in Fig. 1. The  
 576 data in Table 5 was evaluated on the base of 2208 measurements of light vehicles operating in free-  
 577 flow conditions. According to Fig. 6(a), in the case of Ghisalba, only three maneuvers were completely  
 578 measured; in the case of Biella and Poncarale, the number of performance measures per O/D was  
 579 lower than sixteen (four origins per four destinations) since the number of vehicles recorded for certain  
 580 maneuvers (typically the U-turn) was too low.

581  
582**Table 5** Filtered trajectory data for 15th percentile of tortuosity and 85th percentile of operating speed.

Roundabout	O/D	Maneuver	No. of data	$T_{1,15}$ (rad/m <sup>2</sup> )	$T_{2,15}$ (rad/m)	$V_{1,85}$ (km/h)	$V_{2,85}$ (km/h)	$V_{3,85}$ (km/h)
------------	-----	----------	-------------	-------------------------------------	-----------------------	----------------------	----------------------	----------------------

Biella 1C	2-3	Right turn	20	0.00124	0.0311	32.27	34.07	39.37
	2-5	Crossing	185	0.00015	0.0096	33.88	39.00	44.11
	4-1	Left turn	21	0.00200	0.0372	29.58	27.75	40.55
	4-5	Right turn	50	0.00129	0.0330	29.33	30.44	33.62
	4-7	Crossing	73	0.00069	0.0216	30.61	36.09	41.38
	6-1	Crossing	185	0.00094	0.0255	32.71	33.43	42.68
	6-3	Left turn	42	0.00207	0.0383	33.70	29.52	42.43
	6-7	Right turn	83	0.00064	0.0218	34.63	34.66	37.27
	8-1	Right turn	20	0.00054	0.0207	31.89	33.08	37.88
	8-3	Crossing	72	0.00041	0.0163	36.11	35.51	44.56
Ghisalba 3C-BI	8-5	Left turn	97	0.00179	0.0336	33.56	27.81	39.64
	2-3	Right turn	33	0.00047	0.0204	34.15	36.27	35.52
	2-5	Crossing	364	0.00070	0.0224	36.70	35.80	40.07
Ghisalba 3C-MT	4-5	Right turn	9	0.00032	0.0168	35.25	38.66	40.76
	2-3	Right turn	33	0.00050	0.0203	30.70	32.90	33.67
	2-5	Crossing	364	0.00067	0.0221	36.41	35.83	40.22
Poncarale 2C-BI	4-5	Right turn	9	0.00037	0.0182	31.57	34.61	39.18
	4-1	Left turn	42	0.00077	0.0241	43.60	37.70	47.02
	4-7	Crossing	183	0.00035	0.0152	40.26	39.59	46.31
	2-3	Right turn	22	0.00100	0.0298	32.43	32.71	38.91
	2-7	Left turn	28	0.00075	0.0233	34.67	35.47	44.92
	8-3	Crossing	226	0.00048	0.0177	37.76	38.03	45.25
	8-1	Right turn	47	0.00007	0.0065	39.09	44.88	49.48

583

584

The 85th percentile of speed distribution is widely considered in the geometric design of highways.

585

It is compared with the design speed to assess speed consistency between the hypothesis of

586

designer and driver behaviour. It reflects the movement of isolated vehicles (i.e., free-flow conditions),

587

and separates the population of prudent drivers from the group of more aggressive ones (Yasser and

588

Mohamed, 2011).

589

The choice of the two percentiles is based on the supposition that aggressive drivers, whose

590

speeds exceed the 85th percentile, tend to follow the fastest path that should be characterized by the

591

lowest tortuosity (as also suggested in Rodegerdts et al., 2007, 2010). The authors associated the

592

15th percentile of tortuosity indexes with the fastest path so as to establish correlations between

593

trajectory and speeds.

594

When the analysis is confined to a part of the speed data, the most significant relationships

595

between the values reported in Table 5 are limited to the 85th percentile of speeds calculated at the

596 middle point of trajectories ( $V_{2,85}$ ) and the 15th percentile of the two tortuosity indexes  $T_{1,15}$  and  $T_{2,15}$ .  
 597 The results are reported in Figs. 7 and 8, and demonstrate that  $T_{2,15}$  rather than  $T_{1,15}$  has a rather good  
 598 correlation to  $V_{2,85}$  as confirmed by the statistics of the two models summarized in Table 6.

599 Figs. 7 and 8 also report the data generated with the MT strategy in the case of the Ghisalba  
 600 roundabout. These data are more dispersed when compared to the corresponding data derived with  
 601 the BI strategy, and, as a consequence, they were not taken into account in the exponential model  
 602 which was plotted in both figures, and which exhibited the highest coefficient of determination for both  
 603 tortuosity indexes.

604 Very low correlation values were found between the 85th percentile of entry ( $V_1$ ) and exit ( $V_3$ )  
 605 speeds. This may be attributed to the fact that the entry speed largely depends on driver behaviour in  
 606 the approaching leg, while the exiting speed depends more on the specific shape of curbs around the  
 607 exit lane.

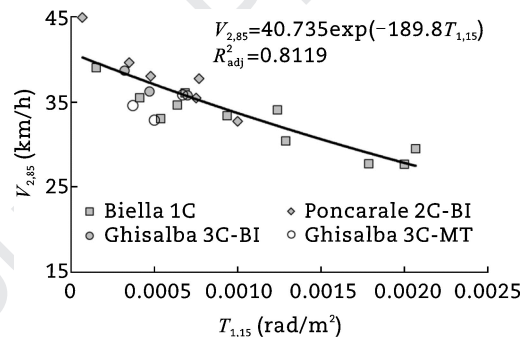


Fig. 7 Relationship between  $V_{2,85}$  and  $T_{1,15}$  index.

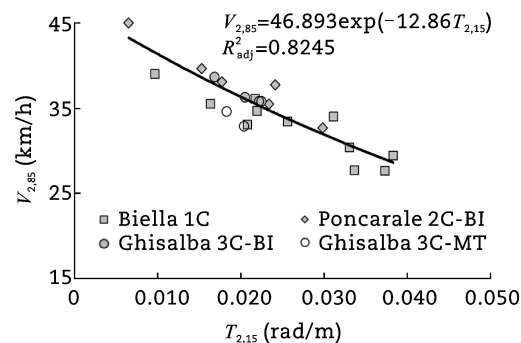


Fig. 8 Relationship between  $V_{2,85}$  and  $T_{2,15}$  index.

Table 6 Output of statistics for model reported in Figs. 7 and 8.

Model	$V_{2,85} = 40.735\exp(-189.8T_{1,15})$	$V_{2,85} = 46.893\exp(-12.86T_{2,15})$
-------	---	---

608  
 609  
 610  
 611  
 612

613  
 614  
 615  
 616  
 617

$R^2$		0.8218	0.8337
$R^2$ adjusted		0.8119	0.8245
Standard error		0.0520	0.0510
$F$ value		83.0259	90.2644
		( $F$ critical = 2.17, $p$ = 0.05)	( $F$ critical = 2.17, $p$ = 0.05)
$p$ value	Intercept	$1.27 \times 10^{-30}$	$2.90 \times 10^{-27}$
	Variable	$3.66 \times 10^{-8}$	$1.95 \times 10^{-8}$

618

619 It must be stressed that we limited the study of correlation between speed and tortuosity only to  
620 three points (entry, middle and exit) as reproduction of the approach proposed by Rodegerdts et al.  
621 (2007).

#### 622 5.4 Acceleration analysis

623 Table 7 shows the statistics for acceleration and deceleration measured on the circulatory roadway for  
624 the Ghisalba and Poncarale roundabouts (trajectory data are the same of Table 5). It should be  
625 highlighted once again that the data considered here pertain to vehicles that were not affected by  
626 other vehicles when negotiating the roundabout, thus all the data can be considered to be that of  
627 isolated vehicles and drivers affected by the roundabout geometrics only.

628 According to the speed variation model depicted in Fig. 1, the deceleration from sections 1 to 2 is  
629 indicated as  $a_{12}$ , while the acceleration from the central point of the trajectory (section 2) to the exit  
630 section (section 3) is indicated as  $a_{23}$ .

631  
632

**Table 7** Statistics for vehicular acceleration and deceleration at the Ghisalba and Poncarale roundabouts.

Roundabout	Ghisalba 3C-BI				Poncarale 2C-BI					
	Right turn		Through		Right turn		Through		Left turn	
Acceleration	$a_{12}$	$a_{23}$	$a_{12}$	$a_{23}$	$a_{12}$	$a_{23}$	$a_{12}$	$a_{23}$	$a_{12}$	$a_{23}$
No. of objects	42	42	364	364	69	69	409	409	70	70
Mean (m/s <sup>2</sup> )	-0.614	0.116	-0.063	0.409	-0.674	0.719	-0.264	0.468	-0.051	0.358
Standard deviation (m/s <sup>2</sup> )	0.601	0.499	0.370	0.273	1.030	0.660	0.555	0.616	0.312	0.204
15th percentile (m/s <sup>2</sup> )	-1.241	-0.556	-0.378	0.142	-1.724	0.117	-0.831	0.141	-0.371	0.205
85th percentile (m/s <sup>2</sup> )	-0.038	0.606	0.281	0.676	0.132	1.261	0.235	0.744	0.257	0.543
Max (m/s <sup>2</sup> )	0.213	1.075	1.160	1.204	3.037	2.796	2.228	11.141	0.838	0.739

Min (m/s <sup>2</sup> )	-1.901	-0.721	-1.948	-0.793	-3.201	-1.474	-2.156	-0.832	-0.895	-0.518
-------------------------	--------	--------	--------	--------	--------	--------	--------	--------	--------	--------

633

634 Per each vehicle traversing the roundabout, these two values were computed with the following  
635 equations.

$$636 \quad a_{12} = (v_{22} - v_{12}) / (2d_{12}) \quad (10)$$

$$637 \quad a_{23} = (v_{32} - v_{22}) / (2d_{23}) \quad (11)$$

638 where  $d_{12}$  and  $d_{23}$  have the same meaning of Eqs. (1) and (2). Data have also been distinguished for  
639 left turn, right turn, and through movements.

640 The mean and the standard deviation of acceleration values indicate that entering vehicles in  
641 deceleration ( $a_{12}$ ) and exiting vehicles in acceleration ( $a_{23}$ ) exhibit large variations as a result of the  
642 roundabout layout and geometrics, and type of maneuvers. The 15th percentiles of deceleration ( $a_{12}$ ),  
643 listed in Table 7, are only higher in the case of right turn movements than the absolute value of 1.3  
644 m/s<sup>2</sup> suggested in Rodegerdts et al. (2007), and reflect the behaviour of aggressive drivers. In all  
645 other cases, the statistics for  $a_{12}$  indicate that lower values are observed.

646 Regarding the acceleration variable ( $a_{23}$ ), a large difference is evident between the observed values  
647 and the value of 2.3 m/s<sup>2</sup> proposed again in Rodegerdts et al. (2007), thus suggesting the need for an  
648 extended investigation into a greater number of roundabout geometry types. In fact, the two  
649 roundabouts considered here yield different results as a consequence of the significant difference in  
650 their layout.

## 651 **6 Discussion**

652 The results illustrated in previous paragraphs outlined the strengths and weaknesses associated with  
653 each set-up for the three different roundabouts considered in the investigation. In the three cases,  
654 small camera oscillations, clouds, and flying objects (i.e., birds) affecting image quality were easily  
655 identified and corrected.

656 On examination of the three configurations presented in Fig. 4, it is clear that the central position of  
657 the video cameras facilitates a reduction in perspective distortion but, as in the case of Ghisalba  
658 (configuration #2 in Fig. 4 with three cameras), a relatively high number of video cameras is required

659 given the dimensions of the circulatory roadway. The blending of images becomes more complicated  
660 with an increase in the number of video cameras installed at or around the roundabout. Moreover,  
661 synchronization between cameras becomes crucial: with the loss of only one frame of a video camera  
662 necessitating a challenging task of realignment between video frames.

663 Elevated vantage points on poles or buildings introduce high levels of distortion especially in the  
664 case of heavy and long vehicles, as in the case of Poncarale (configuration #3 in Fig. 4 with three  
665 cameras). Furthermore, the height of vantage points has a detrimental impact on image quality since  
666 the cameras and their supports are exposed to stronger winds, which can produce oscillations that are  
667 hard to correct during the image treatment phase. From an analysis of the data collected at the  
668 Poncarale roundabout, it would appear that the merging of trajectories extracted from different images  
669 (MT strategy) seems to be less effective than the blending images (BI) technique. In this case, the  
670 only one for which this comparison has been made, the performance indicators associated with the  
671 evaluation of the O/D matrix indicate a greater dispersion of data in the case of the merged trajectory  
672 technique (Table 5).

673 Whereas the blending of images is essentially a straightforward task when video cameras have  
674 viewing angles of less than  $90^\circ$ , it tends to prove problematic with wider angles (especially those  
675 closer to  $180^\circ$ ) as a consequence of the different perspective distortions of moving elements. Of the  
676 three configurations considered in this research, the use of a single video camera mounted on a pole  
677 located outside the roundabout, as in the case of Biella (with the camera located at the external side  
678 of the circulatory roadway), would appear to offer the best compromise in terms of survey costs,  
679 pre-processing work, and quality of results. However, this is not a definitive conclusion, since the  
680 number of experiments carried out to date is not considered comprehensive from a technological point  
681 of view. In this study, the authors focused primarily on a general evaluation of the methodology and  
682 the estimation of technical problems to be solved for each specific configuration. In fact, while the  
683 results here have been used to assess the survey methodology, they cannot be considered  
684 statistically significant in terms of the performances of the investigated roundabouts or, indeed,  
685 roundabouts in general.

686 In all the three configurations depicted in Fig. 4, VeTRA has been able to collect spatial and  
687 temporal data for a large number of points along each trajectory, thus deriving local speeds. The  
688 authors decided to consider speeds at the entry gate, at the midpoint and at the exit of the roundabout  
689 to compare results with those in Rodegerdts et al. (2007). Two different tortuosity indexes were  
690 calculated for each trajectory by combining angular deviation and the distance between two  
691 successive recorded points, and the radius of the local osculating circle in different ways.

692 As a result, some linear and exponential relationships between the 85th percentile of speeds and  
693 the 15th percentile of tortuosity indexes have been derived. The observations confirm that an effective  
694 speed control within the circulatory roadway is possible only when high horizontal curvatures of  
695 vehicle paths (i.e., high values of tortuosity) are achieved as a consequence of the combination of the  
696 geometric characteristics of roundabout elements.

697 The regression equations presented here were obtained from 2208 speed data (Table 5) of just  
698 three roundabouts with each exhibiting a different geometry in terms of external and central island  
699 diameters, circulatory roadway width, number and geometry of entry and exit lanes. The high  
700 coefficient of determination of one of the four proposed equations ( $R^2 = 0.8337$  for the exponential  
701 relationship between  $V_{2,85}$  and the  $T_{2,15}$ ) facilitates its use in the estimation of the circulating operating  
702 speed ( $V_{2,85}$ ) in the analysis and design of roundabouts.

703 Acceleration and deceleration values on the circulatory roadways exhibit large variations as a  
704 consequence of roundabout layout and geometrics, maneuver type, and driving attitudes and styles.  
705 In light of the observation data, the suggested values of  $-1.3 \text{ m/s}^2$  in deceleration and  $2.1 \text{ m/s}^2$  in  
706 acceleration included in the NCHRP Reports 572 and 672 (Rodegerdts et al., 2007, 2010) seem to be  
707 questionable, thus new research is necessary to obtain better design-operating speed and  
708 acceleration distribution on the circulatory roadway. This paper has demonstrated that image analysis  
709 has the potential to achieve such objectives.

710

711

712

## 713 7 Conclusions

714 The paper presents the results of several activities undertaken involving extensive use of the VeTRA  
715 software and acquisition tools, which the authors developed for the specific purpose of carrying out  
716 operational analyses of roundabouts through the use of video-tracking technology.

717 At present, the comprehensive gathering of operational data at roundabouts necessitates the use of  
718 non-integrated acquisition systems and prolonged data analysis times. Since 2010, the authors have  
719 worked on the development of an integrated system (specifically designed for roundabouts)  
720 composed of a hardware system for data acquisition and collection, and software for data analysis.

721 The system and some data analysis have already been presented in previous referenced works  
722 (Mussone et al., 2011, 2013), in which the system included one video camera only.

723 In this paper, the authors focused their attention on an extended use of the software with the aims  
724 of solving issues related to the survey configuration used with more than one video camera and their  
725 positioning inside or around the roundabout, and improving the tracking system of vehicles and  
726 deriving the O/D matrix and trajectories (i.e., position and time of tracked vehicles).

727 Two possible strategies consisting in (a) the merging of trajectories extracted from each separate  
728 video, and (b) the image blending from different video cameras before extracting trajectories were  
729 investigated. Results suggest that the second is more effective than the first one. Furthermore, of the  
730 three configurations considered, the one consisting in a single video camera mounted on a pole  
731 outside the roundabout appeared to be the optimal in terms of costs, processing work, and quality of  
732 results. However, this solution may imply large perspective distortion of the tracked vehicles in  
733 locations far from the camera, especially in case of roundabout with large diameters. To limit  
734 perspective distortion, the vantage point must be raised up as much as possible.

735 From the data collected from case studies, one further result concerns the correlation between  
736 speed and tortuosity of vehicle trajectories, which could be used by designers in the estimation of  
737 vehicle performance when negotiating a roundabout. This result emphasizes the tremendous potential  
738 of the image analysis in capturing position and kinematic of vehicles, and opens up to further studies  
739 on the evaluation of the operational effects of roundabouts.

740 In conclusion, previous works by the authors, together with the results reported in this paper, testify  
741 to the fact that the video survey system and the processing code are both robust and reliable. As  
742 documented in this paper, the authors are aware that further work is necessary to improve the  
743 performance of the tracking system of VeTRA in all possible set-up configurations.

744 With this objective in mind, a new version of the software is under development. It will include a set  
745 of 3D models of vehicles that differ in terms of dimensions and that can be associated with each blob.  
746 In this way, trajectories will be derived with reference to the geometric centre of the model rather than  
747 to the centre of the blob. This approach, already adopted by some authors but in different road  
748 scenarios (Kim et al., 2005; Koller et al., 1993; Messelodi et al., 2005), can lead to better vehicle  
749 recognition, which is considerable when high perspective distortions are present (like in Poncarale),  
750 together with even more precise localization and tracking. The authors are confident that the use of  
751 vehicle models will reduce the negative effect of video camera oscillations and will enable the  
752 separation of the shadows (of vehicles) from the actual vehicles in blobs, thus reducing the impact of  
753 shadows on the quality of collected data. Finally, to extend the possibility of data collection to night-  
754 time conditions, new research will also be carried out assessing how to use videos from thermal  
755 and/or infra-red video cameras.

#### 756 **Conflict of interest**

757 The authors do not have any conflict of interest with other entities or researchers.

#### 758 **References**

- 759 Ahac, S., Džambas, T., Dragčević, V., 2016. Review of fastest path procedures for single-lane  
760 roundabouts. In: The 4th International Conference on Road and Rail Infrastructure (CETRA),  
761 Sibenik, 2016.
- 762 Alhajyaseen, W.K.M., Asano, M., Nakamura, H., et al., 2013. Stochastic approach for modeling the  
763 effects of intersection geometry on turning vehicle paths. *Transportation Research Part C:*  
764 *Emerging Technologies* 32, 179-192.

- 765 Apeltauer, J., Babinec, A., Herman, D., et al., 2015. Automatic vehicle trajectory extraction for traffic  
766 analysis from aerial video data. *The International Archives of Photogrammetry, Remote Sensing*  
767 *and Spatial Information Sciences* 40(3), 9.
- 768 Autodesk, 2018. Civil 3D: Civil Infrastructure Design and Documentation Software. Available at:  
769 <https://www.autodesk.com/products/civil-3d/overview> (Accessed 10 September 2019).
- 770 Bernardin, K., Stiefelhagen, R., 2008. Evaluating multiple object tracking performance: the CLEAR  
771 MOT metrics. *EURASIP Journal on Image and Video Processing* 2008, 1-10.
- 772 Beymer, D., McLauchlan, P., Coifman, B., et al., 1997. A real-time computer vision system for  
773 measuring traffic parameters. In: *IEEE Computer Society Conference on Computer Vision and*  
774 *Pattern Recognition*, San Juan, 1997.
- 775 Curti, V., Marescotti, L., Mussone, L., 2008. *Roundabouts: Design and Evaluations of Roundabout*  
776 *Intersections*, fourth ed. Maggioli, Ravenna.
- 777 Datondji, S.R.E., Dupuis, Y., Subirats, P., et al., 2016. A survey of vision-based traffic monitoring of  
778 road intersections. *IEEE Transactions on Intelligent Transportation Systems* 17(10), 2681-2698.
- 779 Dinh, H., Tang, H., 2017. A video processing system for automated traffic data collection of gap size  
780 for roundabouts. In: *IEEE 30th Canadian Conference on Electrical and Computer Engineering*,  
781 Windsor, 2017.
- 782 Fernandes, P., Salamati, K., Roupail, N.M., et al., 2015. Identification of emission hotspots in  
783 roundabouts corridors. *Transportation Research Part D: Transport and Environment* 37, 48-64.
- 784 Grenard, J.L., Wei, T., 2012. *Traffic Counting at Roundabouts Using Video Technology: A*  
785 *Practitioner's View-White Paper*. Available at: <http://miovision.com/white-papers-research-reports/>  
786 (Accessed 2 March 2014).
- 787 Guido, G., Gallelli, V., Rogano, D., et al., 2016. Evaluating the accuracy of vehicle tracking data  
788 obtained from unmanned aerial vehicles. *International Journal of Transportation Science and*  
789 *Technology* 5(3), 136-151.
- 790 Kim, Z.W., Gomes, G., Hranac, R., et al., 2005. A machine vision system for generating vehicle  
791 trajectories over extended freeway segments. In: *12th World Congress on Intelligent*  
792 *Transportation Systems*, San Francisco, 2005.

- 793 Koller, D., Daniilidis, K., Nagel, H.H., 1993. Model-based object tracking in monocular image  
794 sequences of road traffic scenes. *International Journal of Computer Vision* 10(3), 257–281.
- 795 Messelodi, S., Modena, C.M., Zanin, M., 2005. A computer vision system for the detection and  
796 classification of vehicles at urban road intersections. *Pattern Analysis and Applications* 8(1-2), 17-  
797 31.
- 798 Migliore, D.A., Matteucci, M., Naccari, M., 2006. A reevaluation of frame difference in fast and robust  
799 motion detection. In: *The 4th ACM International Workshop on Video Surveillance and Sensor*  
800 *Networks*, Santa Barbara, 2006.
- 801 Mussone, L., 2013. The analysis of roundabouts through visibility. *Procedia – Social and Behavioral*  
802 *Sciences* 87, 250-268.
- 803 Mussone, L., Matteucci, M., Bassani, M., et al., 2011. Traffic analysis in roundabout intersections by  
804 image processing. In: *The 18th International Federation of Automatic Control (IFAC) World*  
805 *Congress*, Milano, 2011.
- 806 Mussone, L., Matteucci, M., Bassani, M., et al., 2013. An innovative method for the analysis of vehicle  
807 movements in roundabouts based on image processing. *Journal of Advanced Transportation*  
808 47(6), 581–594.
- 809 Oh, J., Min, J., Heo, B., 2012. Development of an integrated system based vehicle tracking algorithm  
810 with shadow removal and occlusion handling methods. *Journal of Advanced Transportation* 46(2),  
811 139–150.
- 812 Perco, P., Marchionna, A., Falconetti, N., 2012. Prediction of the operating speed profile approaching  
813 and departing intersections. *Journal of Transportation Engineering* 138(12), 1476-1483.
- 814 Robinson, B.W., Rodegerdts, L., Scarbrough, W., et al., 2000. *Roundabouts: an Informational Guide*.  
815 FHWA-RD-00-067. Federal Highway Administration, U.S. Department of Transportation,  
816 Washington DC.
- 817 Rodegerdts, L., Blogg, M., Wemple, E., et al., 2006. Appendixes to NCHRP Report 572: Roundabouts  
818 in the United States. NCHRP Web-Only Document 94. Transportation Research Board, National  
819 Research Council, Washington DC.

- 820 Rodegerdts, L., Blogg, M., Wemple, E., et al., 2007. Roundabouts in the United States. NCHRP  
821 Report 572. Transportation Research Board, National Research Council, Washington DC.
- 822 Rodegerdts, L., Bansen, J., Tiesler, C., et al., 2010. Roundabouts: an Informational Guide. NCHRP  
823 Report 672. Transportation Research Board, National Research Council, Washington DC.
- 824 Rodegerdts, L., Jenior, P.M., Bugg, Z.H., et al., 2014. Evaluating the Performance of Corridors with  
825 Roundabouts. NCHRP Report 772. Transportation Research Board, Washington DC.
- 826 Sacchi, E., Bassani, M., Persaud, B., 2011. Comparison of safety performance models for urban  
827 roundabouts in Italy and other countries. *Transportation Research Record* 2265, 253-259.
- 828 Sakshaug, L., Lareshyn, A., Svensson Å., et al., 2010. Cyclists in roundabouts – different design  
829 solutions. *Accident Analysis & Prevention* 42(4), 1338-1351.
- 830 Salamati, K., Coelho, M.C., Fernandes, P., et al., 2013. Emissions estimation at multilane  
831 roundabouts: effects of movement and approach lane. *Transportation Research Record* 2389, 12-  
832 21.
- 833 St-Aubin, P., Saunier, N., Miranda-Moreno, L.F., 2013. Detailed driver behaviour analysis and  
834 trajectory interpretation at roundabouts using computer vision data. *Transportation Research*  
835 *Record* 2389, 65-77.
- 836 Šurdonja, S., Dragčević, V., Deluka-Tibljaš, A., 2018. Analyses of maximum-speed path definition at  
837 single-lane roundabouts. *Journal of Traffic and Transportation Engineering (English Edition)* 5(2),  
838 83-95.
- 839 Suzuki, K., Nakamura, H., 2006. TrafficAnalyzer – the integrated video image processing system for  
840 traffic flow analysis. In: *The 13th Intelligent Transportation Systems World Congress*, London,  
841 2006.
- 842 Transoftsolutions, 2018. TORUS Roundabouts: Roundabout Design Software. Available at:  
843 <https://www.transoftsolutions.com/road-design/torus-roundabouts/> (Accessed 2 January 2019).
- 844 Wei, H., Feng, C., Meyer, E., et al., 2005. Video-capture-based approach to extract multiple vehicular  
845 trajectory data for traffic modeling. *Journal of Transportation Engineering* 131(7), 496-505.
- 846 Yasser, H., Mohamed, S., 2011. Modeling Operating Speed. *Transportation Research Circular*  
847 *Synthesis Report E-C151*. Transportation Research Board, Washington DC.

848 Zaki, M.H., Sayed, T., Cheung, A., 2013. Computer vision techniques for the automated collection of  
849 cyclist data. Transportation Research Record 2387, 10-19.

850



851

852 Marco Bassani, PhD, is an associate professor in roads, railways and airport engineering at the  
853 Politecnico di Torino (Italy) where he teaches "Design of Transportation Infrastructures". In 2014,  
854 he was a visiting professor at the University of Maryland (College Park, US). His main research  
855 interests and publications are related to the use of alternative materials, advanced geometric  
856 design of roads, driving simulation, and road safety. Since 2016, he is in the editorial board of  
857 Transportation Letters: The International Journal of Transportation Research.

858



859

860 Lorenzo Mussone held a master degree in electronic engineering in 1982 and a PhD in  
861 transportation engineering in 1995. Since 2011, he is an associate professor at Politecnico di  
862 Milano. The main scientific activities concern modelling by different techniques: partial derivative  
863 macroscopic equations, microscopic simulation, neural networks, swarm intelligence and graph  
864 theory, applied to road accident data analysis, vehicular flow control, capacity of complex railway  
865 systems, driver behaviour study, roundabouts design, transportation network analysis, and ITS  
866 applications. He is in the panel of reviewers of many transportation journals. Since 2005, he is in  
867 the editorial board of Accident Analysis & Prevention journal and Transportation Research  
868 Interdisciplinary Perspectives.

869

